Optimization of Quantum States for Signaling Across an Arbitrary Qubit Noise Channel With Minimum-Error Detection

François Chapeau-Blondeau

***Abstract*— For discrimination between two signaling states of a qubit, the optimal detector minimizing the probability of error is applied to the situation where detection has to be performed from a noisy qubit affected by an arbitrary quantum noise separately characterized. With no noise, any pair of orthogonal pure quantum states is optimal for signaling as it enables error-free detection. In the presence of noise, detection errors are in general inevitable, and the pairs of signaling states best resistant to such noise are investigated. With an arbitrary quantum noise, modeled as a channel affecting the qubit, and when minimum-error detection is performed from the output, a characterization of the optimal input signaling pairs and of their best detection performance is obtained through a simple maximization of a quadratic scalar criterion in three constrained real variables. This general characterization enables to establish that such optimal signaling pairs are always made of two orthogonal pure quantum states, but that they must be specifically selected to match the noise properties and prior probabilities. The maximization is explicitly solved for several generic quantum noise processes relevant to the qubit, such as the squeezed generalized amplitude damping noise which describes interaction with a thermal bath representing a decohering environment and which includes as special cases both the generalized and the regular amplitude damping noise processes, and such as general Pauli noise processes which include for instance the bit-flip noise and the depolarizing noise. Also, examined is the situation of one imposed (pure or mixed) signaling state, for which the other associated signaling state optimal for noisy detection is determined as a pure state, yet not necessarily orthogonal.**

***Index Terms*— Quantum state discrimination, quantum detection, quantum noise, noisy qubit, decoherence.**

I. Introduction

The discrimination between two alternative quantum states, referred to here as quantum state detection, is a fundamental process of quantum information, relevant for instance to quantum communication, quantum cryptography, quantum measurement [1]–[3]. Except in the special case of two orthogonal quantum states, generally state discrimination cannot be achieved perfectly and has to cope with inevitable error; and such a general situation is frequent since quantum noise and decoherence are prone to break the orthogonality of two initial quantum states. A meaningful general approach then is to seek the optimal quantum measurement protocol, or the optimal detector, enabling discrimination with minimum error. For a given pair of signaling states between which to discriminate, the optimal detector achieving minimal probability of error was characterized in [4]–[6].

The theory of quantum detection introduced in [4]–[6] has been developed in several directions [7]–[15]. We shall use here this theory of optimal quantum detection from [4]–[6], yet within a distinct specific perspective. Most approaches to quantum detection operate with quantum states which are given, as pure or mixed states, and optimal processes are determined directly matched to these given states. As a distinctive specificity, we take here explicitly into account the intervention of some quantum noise, which is separately characterized, and whose characteristics are included as such in the determination of the optimized detection process. This is a common approach in classical signal and information processing, where the optimal processors are usually derived to match a noise which is separately characterized. This perspective is taken here for quantum detection. Instead of two given quantum states directly accessible to the measurement protocol for discrimination, we consider two initial signaling states which can be prepared for a qubit, which are then altered by some quantum noise process before they become accessible to the measurement protocol for discrimination. Such a scenario is specifically relevant to quantum communication, and more broadly to any situation where a quantum system is not directly accessible to measurement but only after alteration by some noise, often representing the action of decoherence through interaction with an uncontrolled environment. The part which is given is the quantum noise process. It describes the unavoidable action of some noise, modeled as channel altering a qubit initially prepared in either of the two states forming the input signaling pair. It is from this noisy version of the qubit, accessible as the output of the noise channel, that state discrimination or binary detection has to be performed efficiently. For a given noise process, we will be interested in determining the optimal initial or input signaling pair of quantum states yielding the best detection performance when minimum-error detection is performed from the noisy qubit. This represents a distinct optimization perspective, stemming from the explicit consideration of a definite quantum

Manuscript received November 17, 2014; revised April 23, 2015; accepted June 2, 2015. Date of publication June 12, 2015; date of current version July 10, 2015.

The author is with the Laboratoire Angevin de Recherche en Ingénierie des Systèmes (LARIS), University of Angers, Angers 49000, France (e-mail: chapeau@univ-angers.fr).

Communicated by M. Grassl, Associate Editor for Quantum Information Theory.

Color versions of one or more of the figures in this paper are available online at http://ieeexplore.ieee.org.

Digital Object Identifier 10.1109/TIT.2015.2445213

noise process characterized separately of the states to be discriminated.

Still another optimization perspective is considered in [16], where this time the quantum measurement protocol is fixed and given, and one seeks the optimal input signaling states rendering this fixed measurement optimal, although with no explicit reference to a quantum noise process involved in the situation. A comparable perspective is also taken in [17], by optimizing input signaling states for quantum communication yet with no noise or for noiseless transmission.

Here, in order to characterize optimization relative to a definite noise process, we consider detection on a qubit. The qubit is a fundamental system of quantum information, and for which general models of quantum noise can be worked out in detail. We thus address minimum-error detection from a noisy qubit. We will first briefly review the theory of minimum-error detection from [4]–[6] and apply it to a noisy qubit, and then introduce the modeling of a general quantum noise on the qubit. A characterization of the optimal signaling pairs of qubit states and their best performance for detection with arbitrary noise will be obtained through a simple maximization problem. This characterization enables to exhibit generic properties of the optimal signaling pairs. In addition, the involved maximization will be explicitly worked out for several quantum noise processes of general relevance to the qubit.

II. Minimum-Error Detection From a Noisy Qubit

Minimum-error quantum detection can be generally characterized as follows [4]–[6]. A quantum system in an N-dimensional Hilbert space $\mathcal{H}_N$, can be in one of two alternative quantum states, represented by two density operators ρ_0 and ρ_1, respectively with prior probabilities P_0 and $P_1 = 1 - P_0$, as a result of its preparation. A general measurement is performed on the system by means of a positive operator-valued measure (POVM) with two elements $\{\mathrm{M}_0, \mathrm{M}_1\}$, so as to obtain a conclusive decision on whether the quantum system is in state ρ_0 or ρ_1. The overall probability of detection error results as $P_{\mathrm{er}} = \mathrm{tr}(\mathrm{M}_1\rho_0)P_0 + \mathrm{tr}(\mathrm{M}_0\rho_1)P_1$. The strategy to minimize P_{er} uses the (Hermitian) test operator $\mathrm{T} = P_1\rho_1 - P_0\rho_0$ to define the optimal measurement as

$$\mathrm{M}_1^{\mathrm{opt}} = \sum_{\lambda_n>0} |\lambda_n\rangle\langle\lambda_n|, \tag{1}$$

expressing that the optimal measurement $\mathrm{M}_1^{\mathrm{opt}}$ to detect ρ_1 is to project on the eigensubspace of T associated with all its positive eigenvalues λ_n; and $\mathrm{M}_0^{\mathrm{opt}} = \mathbb{1} - \mathrm{M}_1^{\mathrm{opt}}$ is the complementary projection, with $\mathbb{1}$ the identity operator on $\mathcal{H}_N$. The optimal POVM $\{\mathrm{M}_0^{\mathrm{opt}}, \mathrm{M}_1^{\mathrm{opt}}\}$ achieves the minimal probability of error expressible as

$$P_{\mathrm{er}}^{\min} = \frac{1}{2}\left(1 - \sum_{n=1}^{N}|\lambda_n|\right) = \frac{1}{2}\Big[1 - \mathrm{tr}(|\mathrm{T}|)\Big]. \tag{2}$$

This minimum-error detection strategy is now applied to the qubit in $\mathcal{H}_2$. In particular, for the qubit, the properties of the test operator T and of the minimum-error detection of Eqs. (1)–(2) can be worked out analytically in detail. The two states for the qubit can be parameterized as [2]

$$\rho_j = \frac{1}{2}\left(\mathbb{1} + \vec{r}_j\vec{\sigma}\right), \qquad j = 0, 1, \tag{3}$$

with the two real 3-dimensional Bloch vectors $\vec{r}_j$ of Euclidean norm $\|\vec{r}_j\| \le 1$, and $\vec{\sigma}$ a vector assembling the three 2×2 Pauli matrices $[\sigma_x, \sigma_y, \sigma_z] = \vec{\sigma}$. For pure states $\|\vec{r}_j\| = 1$ while $\|\vec{r}_j\| < 1$ for mixed states. The test operator $\mathrm{T} = P_1\rho_1 - P_0\rho_0$ for the qubit results as

$$\mathrm{T} = \frac{1}{2}\big[(P_1 - P_0)\mathbb{1} + \vec{t}\,\vec{\sigma}\big], \tag{4}$$

characterized by the test Bloch vector

$$\vec{t} = P_1\vec{r}_1 - P_0\vec{r}_0 = [t_x, t_y, t_z]^\top. \tag{5}$$

The performance of the minimum-error detector of Eqs. (1)–(2) for the qubit then follows as

$$P_{\mathrm{er}}^{\min} = \frac{1}{2}\Big(1 - \|\vec{t}\,\|\Big), \quad \text{when } \|\vec{t}\,\| \ge |P_1 - P_0|, \tag{6}$$

$$P_{\mathrm{er}}^{\min} = \min(P_0, P_1), \quad \text{when } \|\vec{t}\,\| < |P_1 - P_0|. \tag{7}$$

This characterization of the minimum-error detection applies on two given qubit states (ρ_0, ρ_1) supposed directly accessible to measurement. By contrast, for the sequel, we will consider that only noisy versions are accessible after alteration of the qubit by some quantum noise. A quantum noise acting on a qubit affects its state ρ in a way which can be generally represented by a completely positive trace-preserving linear map of the form [2], [3]

$$\rho \longrightarrow \rho' = \mathcal{N}(\rho) = \sum_k \Lambda_k\rho\Lambda_k^\dagger, \tag{8}$$

with the Kraus operators Λ_k (which need not be more than four for the qubit) satisfying $\sum_k \Lambda_k^\dagger\Lambda_k = \mathbb{1}$. Since the transformed, noisy, state $\rho' = \mathcal{N}(\rho)$ remains a density operator of the form of Eq. (3), the map of Eq. (8) can be associated with a transformation of the Bloch vector $\vec{r} \to \vec{r}\,'$ characterizing the alteration of the qubit state.

When detection from the initial noise-free states (ρ_0, ρ_1) was controlled in Eqs. (6)–(7) by the input test vector $\vec{t}$ of Eq. (5), now detection from the noisy states $[\rho_0' = \mathcal{N}(\rho_0), \rho_1' = \mathcal{N}(\rho_1)]$ is controlled by the transformed test vector

$$\vec{t}\,' = P_1\vec{r}_1\,' - P_0\vec{r}_0\,' = [t_x', t_y', t_z']^\top, \tag{9}$$

and the performance of the minimum-error detector of Eqs. (1)–(2) operating on the noisy qubit follows as

$$P_{\mathrm{er}}^{\min} = \frac{1}{2}\Big(1 - \|\vec{t}\,'\|\Big), \quad \text{when } \|\vec{t}\,'\| \ge |P_1 - P_0|, \tag{10}$$

$$P_{\mathrm{er}}^{\min} = \min(P_0, P_1), \quad \text{when } \|\vec{t}\,'\| < |P_1 - P_0|. \tag{11}$$

To minimize the error probability $P_{\mathrm{er}}^{\min}$ of Eqs. (10)–(11), the task is then to select the two signaling states (ρ_0, ρ_1), or equivalently their two Bloch vectors $(\vec{r}_0, \vec{r}_1)$, in order to maximize the norm $\|\vec{t}\,'\|$ of the transformed test vector of Eq. (9). This has to be accomplished in the presence of a given quantum noise model that specifies how the two signaling states (ρ_0, ρ_1) or their two Bloch vectors $(\vec{r}_0, \vec{r}_1)$ determine the transformed test vector $\vec{t}\,'$.

We shall now explicitly address this optimization of the signaling pair (ρ_0, ρ_1) for general quantum noise models on the qubit.

III. General Quantum Noise on the Qubit

An arbitrary noise process acting on the qubit, takes the form of a completely positive trace-preserving quantum operation as in Eq. (8), and can be associated with a transformation of the Bloch vector under the general form [2], [18]

$$\vec{r} \to \vec{r}\,' = \mathrm{A}\vec{r} + \vec{c}, \tag{12}$$

where A is a 3×3 real matrix, and $\vec{c}$ a real vector in $\mathbb{R}^3$. Equation (12) realizes an affine map in $\mathbb{R}^3$ mapping the Bloch sphere (ball) into itself. Further conditions constrain A and $\vec{c}$ to ensure complete positivity, limiting their norm, as discussed in [18]. Here we consider A and $\vec{c}$ as given as the characterization of a valid quantum noise; the required conditions will usually be automatically enforced by consistency of the physical modeling of the noise process constructing A and $\vec{c}$. The transformed test vector of Eq. (9) then follows as

$$\vec{t}\,' = \mathrm{A}\vec{t} + \vec{c}\,', \tag{13}$$

with $\vec{c}\,' = (P_1 - P_0)\vec{c}$.

By the polar decomposition [2], one can write $\mathrm{A} = \mathrm{US}$, where U is a real unitary matrix, and S a real symmetric matrix. The matrix S always has, associated with three eigenvalues (s_1, s_2, s_3), three eigenvectors $\{\vec{s}_1, \vec{s}_2, \vec{s}_3\}$ forming an orthonormal basis of $\mathbb{R}^3$. The transformation of the test vector $\vec{t}$ in Eq. (13) is thus a deformation by S along the axes $\{\vec{s}_1, \vec{s}_2, \vec{s}_3\}$ followed by an isometry U and a translation by $\vec{c}\,'$. The resulting vector $\vec{t}\,'$ has a squared norm expressible as

$$\|\vec{t}\,'\|^2 = \vec{t}\,'^\top \vec{t}\,' = \|\mathrm{A}\vec{t}\,\|^2 + 2\vec{v}^\top \vec{t} + \|\vec{c}\,'\|^2, \tag{14}$$

with the vector $\vec{v} = \mathrm{A}^\top \vec{c}\,'$. Maximizing the performance $P_{\mathrm{er}}^{\min}$ of Eqs. (10)–(11) in minimum-error detection, requires then to maximize the norm $\|\vec{t}\,'\|$, or equivalently $\|\vec{t}\,'\|^2$ in Eq. (14), by proper choice of the two signaling states (ρ_0, ρ_1) or equivalently of their two Bloch vectors $(\vec{r}_0, \vec{r}_1)$. Since $\|\vec{t}\,'\|^2$ in Eq. (14) depends on $(\vec{r}_0, \vec{r}_1)$ only through the input test vector $\vec{t}$ of Eq. (5), maximization of $\|\vec{t}\,'\|^2$ need only be performed according to the components of $\vec{t}$. Also, since the input Bloch vectors $\vec{r}_0$ and $\vec{r}_1$ have at most unit norm, the input test vector $\vec{t}$ of Eq. (5) is constrained by $\|\vec{t}\,\|^2 \le 1$.

Determination of the optimal signaling pair of states for minimum-error detection from a noisy qubit affected by the general noise process of Eq. (12), then amounts to maximizing $\|\vec{t}\,'\|^2$ of Eq. (14) according to the components of $\vec{t}$ of Eq. (5) subject to the constraint $\|\vec{t}\,\|^2 \le 1$. Concerning this maximization, we have Theorem 1:

Theorem 1 (Optimum at Two Orthogonal Pure States): The maximum of $\|\vec{t}\,'\|^2$ in Eq. (14) always occurs at the saturated constraint $\|\vec{t}\,\| = 1$, indicating two orthogonal pure signaling states (ρ_0, ρ_1) at the optimum. □

Proof: Since in Eq. (14) the two terms $\|\mathrm{A}\vec{t}\,\|^2$ and $\|\vec{c}\,'\|^2$ are nonnegative, necessarily at the maximum of $\|\vec{t}\,'\|^2$ the third term $2\vec{v}^\top\vec{t}$ is also nonnegative; if it were negative, the change $\vec{t} \to -\vec{t}$ would increase $\|\vec{t}\,'\|^2$, which is not feasible at the maximum. Consequently, at the maximum of $\|\vec{t}\,'\|^2$ in Eq. (14), necessarily $\|\vec{t}\,\| = 1$; if it were not so, a uniform scaling of $\vec{t}$ to reach $\|\vec{t}\,\| = 1$ would also increase $\|\vec{t}\,'\|^2$, which is not feasible at the maximum. For $\vec{t}$ in Eq. (5), this necessary condition $\|\vec{t}\,\| = 1$ can only be achieved by the choice $\vec{r}_0 = -\vec{r}_1$ and $\|\vec{r}_0\| = \|\vec{r}_1\| = 1$, indicating necessarily two orthogonal pure signaling states (ρ_0, ρ_1) to maximize the performance of minimum-error detection expressed via $\|\vec{t}\,'\|^2$ of Eq. (14). ■

To further determine the optimal $\vec{t}$ maximizing $\|\vec{t}\,'\|^2$ in Eq. (14), it is convenient to express the two vectors $\vec{t} = [t_1, t_2, t_3]^\top$ and $\vec{v} = [v_1, v_2, v_3]^\top$ with their coordinates referring to the orthonormal eigenbasis $\{\vec{s}_1, \vec{s}_2, \vec{s}_3\}$ of S. Then it follows $\|\mathrm{A}\vec{t}\,\|^2 = \|\mathrm{S}\vec{t}\,\|^2 = \sum_{k=1}^3 s_k^2 t_k^2$ establishing Theorem 2:

Theorem 2 (Maximization in Eigenbasis): The maximization problem of Eq. (14) can be expressed in the orthonormal eigenbasis $\{\vec{s}_1, \vec{s}_2, \vec{s}_3\}$ of S as

$$\max_{\vec{t}} \left[J(\vec{t}\,) = \sum_{k=1}^{3} \Big(s_k^2 t_k^2 + 2v_k t_k \Big) \right], \tag{15}$$

$$\text{subject to } \|\vec{t}\,\|^2 = \sum_{k=1}^{3} t_k^2 = 1. \tag{16}$$

□

A solution $\vec{t} = \vec{t}^{\,\mathrm{opt}}$ solving the maximization of Theorem 2, defines the optimal signaling pair of pure states $(\rho_0^{\mathrm{opt}}, \rho_1^{\mathrm{opt}})$ by $(\vec{r}_0 = -\vec{t}^{\,\mathrm{opt}}, \vec{r}_1 = \vec{t}^{\,\mathrm{opt}})$, maximizing the performance in minimum-error detection from the noisy qubit. Closed-form solution to the maximization of Theorem 2 is not easily accessible in general. For resolution, one can for instance use Eq. (16) to obtain $t_3^2 = 1 - t_1^2 - t_2^2$ so as to eliminate t_3 in Eq. (15) and then perform a maximization of Eq. (15) in (t_1, t_2) over the unit disk $t_1^2 + t_2^2 \le 1$. Alternatively, one can define a Lagrangian $\mathcal{L}$ for the system of Eqs. (15)–(16) as $\mathcal{L} = J(\vec{t}\,) + \xi(\|\vec{t}\,\|^2 - 1)$ with Lagrange multiplier ξ. The stationarity condition $\partial\mathcal{L}/\partial t_k = 0$ yields $t_k = -v_k/(s_k^2 + \xi)$, for $k = 1, 2, 3$; this put in the constraint $\|\vec{t}\,\|^2 = 1$ then yields an equation in the remaining sole unknown ξ. Yet, none of these two approaches allows to reach closed-form solution in general. However, special matrices A and vectors $\vec{c}$ characterizing in Eq. (12) specific noise processes of significant interest for the qubit, lead to closed-form analytic solutions as we shall see in the sequel. In addition, numerical resolution of Eqs. (15)–(16) can always be performed for any given A and $\vec{c}$.

There also exist special configurations where the solution to the maximization of Theorem 2 can be further specified in general terms. In particular, for any noise with $\vec{c} = \vec{0}$ in Eq. (12), or when $P_0 = P_1 = 1/2$, the optimal $\vec{t}$ maximizing $\|\vec{t}\,'\|^2$ in Eq. (14), or equivalently solving Eqs. (15)–(16), is a unit vector $\vec{t}^{\,\mathrm{opt}}$ pointing in the direction of the eigenvector $\vec{s}_k$ having the eigenvalue with maximum modulus $|s_k|$, and it achieves the maximum $\|\vec{t}\,'\|_{\max} = |s_k|$ to be used in Eqs. (10)–(11) to express the best detection performance. This $\vec{t}^{\,\mathrm{opt}}$ defines the optimal signaling pair $(\rho_0^{\mathrm{opt}}, \rho_1^{\mathrm{opt}})$ by $(\vec{r}_0 = -\vec{t}^{\,\mathrm{opt}}, \vec{r}_1 = \vec{t}^{\,\mathrm{opt}})$, modulo the change $\vec{t}^{\,\mathrm{opt}} \to -\vec{t}^{\,\mathrm{opt}}$ for an equivalent solution, maximizing the performance in minimum-error detection from the noisy qubit.

IV. SQUEEZED GENERALIZED AMPLITUDE DAMPING NOISE

A sophisticated and physically motivated noise process that can affect a qubit is the squeezed generalized amplitude damping noise (SGAD) [19]–[21]. Such a noise process describes the interaction, in various configurations, of the qubit with an uncontrolled environment represented by a thermal bath. The SGAD noise includes as special cases both the generalized and the regular amplitude damping noise processes [2], [22]. The SGAD quantum noise can be modeled, in Eq. (8), by the four Kraus operators [19]–[21]

$$\Lambda_0 = \sqrt{p}\begin{bmatrix} \sqrt{1-\mu} & 0 \\ 0 & \sqrt{1-\nu} \end{bmatrix}, \tag{17}$$

$$\Lambda_1 = \sqrt{p}\begin{bmatrix} 0 & \sqrt{\nu} \\ \sqrt{\mu}e^{-i\Phi} & 0 \end{bmatrix}, \tag{18}$$

$$\Lambda_2 = \sqrt{1-p}\begin{bmatrix} \sqrt{1-\alpha} & 0 \\ 0 & 1 \end{bmatrix}, \tag{19}$$

$$\Lambda_3 = \sqrt{1-p}\begin{bmatrix} 0 & 0 \\ \sqrt{\alpha} & 0 \end{bmatrix}, \tag{20}$$

with the real parameters μ, ν, α and p all in $[0, 1]$, and Φ a phase in $[0, 2\pi)$, with more detail concerning the physical parameters of the SGAD noise given in the Appendix. The associated affine map in Eq. (12) follows with

$$\mathrm{A} = \begin{bmatrix} a_{xx} & a_{xy} & 0 \\ a_{xy} & a_{yy} & 0 \\ 0 & 0 & a_{zz} \end{bmatrix}, \tag{21}$$

and

$$\vec{c} = [0, \quad 0, \quad c_z]^\top, \tag{22}$$

with the components

$$a_{xx} = p[\sqrt{1-\mu}\sqrt{1-\nu} + \cos(\Phi)\sqrt{\mu\nu}] + (1-p)\sqrt{1-\alpha}, \tag{23}$$

$$a_{yy} = p[\sqrt{1-\mu}\sqrt{1-\nu} - \cos(\Phi)\sqrt{\mu\nu}] + (1-p)\sqrt{1-\alpha}, \tag{24}$$

$$a_{xy} = -p\sin(\Phi)\sqrt{\mu\nu}, \tag{25}$$

$$a_{zz} = 1 - p(\mu+\nu) - (1-p)\alpha, \tag{26}$$

$$c_z = -p(\mu-\nu) - (1-p)\alpha. \tag{27}$$

Since A in Eq. (21) is already a real symmetric matrix, then $\mathrm{A} \equiv \mathrm{S}$, and the eigenvalues of S are $s_1 = s_+$, $s_2 = s_-$ and $s_3 = a_{zz}$, with

$$s_\pm = \frac{1}{2}\left(a_{xx} + a_{yy} \pm \sqrt{\Delta}\right), \tag{28}$$

and the discriminant of the characteristic equation $\Delta = (a_{xx} - a_{yy})^2 + 4a_{xy}^2 = 4p^2\mu\nu$, from the expressions of the components of A in Eqs. (23)–(25). Also, in this way

$$s_\pm = p\left(\sqrt{1-\mu}\sqrt{1-\nu} \pm \sqrt{\mu\nu}\right) + (1-p)\sqrt{1-\alpha}. \tag{29}$$

The associated eigenvectors of $\mathrm{A} \equiv \mathrm{S}$ are $\vec{s}_1 = \vec{s}_+$, $\vec{s}_2 = \vec{s}_-$ and $\vec{s}_3 = [0, 0, 1]^\top$, with

$$\vec{s}_\pm = \left[1, \frac{a_{yy} - a_{xx} \pm \sqrt{\Delta}}{2a_{xy}}, 0\right]^\top \tag{30}$$

prior to normalization. From the expressions of the components of A in Eqs. (23)–(25), one finally obtains the two normalized eigenvectors

$$\vec{s}_1 = \vec{s}_+ = [\cos(\Phi/2), -\sin(\Phi/2), 0]^\top, \tag{31}$$

$$\vec{s}_2 = \vec{s}_- = [\sin(\Phi/2), \cos(\Phi/2), 0]^\top. \tag{32}$$

This demonstrates that the eigenvectors (31)–(32) of the SGAD noise transformation A are only influenced by the squeezing angle Φ as introduced in Eq. (A-1), simply oriented by $\Phi/2$ in the plane (Ox, Oy), and are not influenced by its other parameters in Eqs. (A-2)–(A-5) which on the contrary affect the eigenvalues of Eq. (29).

For the SGAD quantum noise performing the affine transformation of Eq. (13) with $(\mathrm{A}, \vec{c})$ given from Eqs. (21)–(22), the solution to Eqs. (15)–(16) can be obtained through a geometric characterization as follows. The Bloch sphere assimilated in $\mathbb{R}^3$ to the points $\vec{t}$ satisfying $\|\vec{t}\| = 1$ is deformed by A into an ellipsoid, by compression along the Oz axis and along the two orthogonal directions defined by $(\vec{s}_1, \vec{s}_2)$ of Eqs. (31)–(32) in the plane (Ox, Oy); then this ellipsoid is translated by $c_z' = (P_1 - P_0)c_z$ along the Oz axis. The resulting transformed points denoted by $\vec{t}\,'$ will lead to the maximum norm $\|\vec{t}\,'\|$ according to the following conditions.

When the eigenvalue $s_3 = a_{zz}$ has the maximum modulus, i.e. $|s_3| = \max(|s_1|, |s_2|, |s_3|)$, then the extension is maximum in the Oz direction for the ellipsoid after compression by A of Eq. (21). The maximum extension $|s_3| = |a_{zz}|$ of the ellipsoid added to the translation c_z' in the Oz direction, defines the $\vec{t}\,'$ with maximal norm, occurring in the Oz direction with $\|\vec{t}\,'\|_{\max} = |a_{zz}| + |c_z'|$. Such a $\vec{t}\,'$ in the Oz direction with maximal norm $\|\vec{t}\,'\|_{\max} = |a_{zz}| + |c_z'|$, is achieved by transforming $\vec{t} = [0, 0, 1]^\top$ when $a_{zz}c_z' > 0$ or $\vec{t} = [0, 0, -1]^\top$ when $a_{zz}c_z' < 0$. This determines a unique optimal input test vector $\vec{t} = \vec{t}^{\,\mathrm{opt}}$ characterizing a unique optimal signaling pair $(\rho_0^{\mathrm{opt}} = |1\rangle\langle 1|, \rho_1^{\mathrm{opt}} = |0\rangle\langle 0|)$ when $a_{zz}c_z' > 0$ or $(\rho_0^{\mathrm{opt}} = |0\rangle\langle 0|, \rho_1^{\mathrm{opt}} = |1\rangle\langle 1|)$ when $a_{zz}c_z' < 0$. This optimal signaling pair maximizes the performance of Eqs. (10)–(11) in minimum-error detection from the noisy qubit altered by the SGAD noise, with $|a_{zz}|$ large enough.

However, a more generic situation for the SGAD noise is with smaller $|a_{zz}|$. When $s_3 = a_{zz}$ is not the eigenvalue of A with maximum modulus, then it is necessarily $s_1 = s_+ > 0$ from Eq. (29) which is the eigenvalue with maximum modulus. In the compression by A of the Bloch sphere, the resulting ellipsoid has thus a maximal extension $s_1 = s_+ > 0$ occurring in the direction defined by the eigenvector $\vec{s}_1 = \vec{s}_+$ in Eq. (31). When the translation by c_z' along the Oz axis is performed on the ellipsoid, the point $\vec{t}\,'$ resulting with maximal norm $\|\vec{t}\,'\|_{\max}$ is necessarily obtained by transforming through Eq. (13) an input unit vector $\vec{t}$ lying in the plane defined by $\vec{s}_1$ and Oz, and that can be parameterized in the orthonormal eigenbasis $\{\vec{s}_1, \vec{s}_2, \vec{s}_3 \parallel Oz\}$ as $\vec{t} = [t_1, 0, t_3 = t_z]^\top$. Any $\vec{t}$ outside this plane $(\vec{s}_1, Oz)$ would be transformed by A into a vector with a component of shorter norm in the plane (Ox, Oy), and finally into a $\vec{t}\,'$ with shorter global norm $\|\vec{t}\,'\|$ when the component along Oz (carrying the effect of the translation along Oz) is included. Now for $\vec{t} = [t_1, 0, t_3 = t_z]^\top$, since $\vec{v} = [0, 0, a_{zz}c'_z]^\top$, one obtains from Theorem 2 the maximization problem

$$\max_{\vec{t}} \Big[J(\vec{t}) = s_1^2 t_1^2 + a_{zz}^2 t_z^2 + 2a_{zz}c'_z t_z \Big], \tag{33}$$

$$\text{subject to } \|\vec{t}\|^2 = t_1^2 + t_z^2 = 1. \tag{34}$$

The maximization of Eqs. (33)–(34) can be solved by a Lagrange multiplier approach; or by substitution of $t_1^2 = 1 - t_z^2$ in Eq. (33) one obtains $J(\vec{t}) = J(t_z) = -(s_1^2 - a_{zz}^2)t_z^2 + 2a_{zz}c'_z t_z + s_1^2$ having a maximum at $t_z = a_{zz}c'_z/(s_1^2 - a_{zz}^2)$, which is sufficient for an unconstrained maximization of $J(t_z)$ but not necessarily the solution to Eqs. (33)–(34) since also $t_z \in [-1, 1]$ is required. When $t_z = a_{zz}c'_z/(s_1^2 - a_{zz}^2) \in [-1, 1]$, this defines the solution to Eqs. (33)–(34) together with $t_1 = \pm\sqrt{1 - t_z^2}$ determining two equivalent maxima of $J(\vec{t})$; in this configuration, over the circle defined by $t_1^2 + t_z^2 = 1$, $J(t_1, t_z)$ in Eq. (33) describes a closed loop with a saddle profile with the two equivalent maxima described above, and also two local minima at $(t_1 = 0, t_z = \pm 1)$. When $t_z = a_{zz}c'_z/(s_1^2 - a_{zz}^2) \notin [-1, 1]$, $J(t_1, t_z)$ in Eq. (33) describes a closed loop with the profile of a tilted ring, with a single maximum at $(t_1 = 0, t_z = 1)$ if $a_{zz}c'_z > 0$ or at $(t_1 = 0, t_z = -1)$ if $a_{zz}c'_z < 0$, and a single minimum respectively at $(t_1 = 0, t_z = -1)$ or $(t_1 = 0, t_z = 1)$. This solves the maximization of Eqs. (33)–(34) with solutions $\vec{t} = \vec{t}^{\,\text{opt}}$ characterized in the parameterization $\vec{t} = [t_1, 0, t_3 = t_z]^\top$ referring to the eigenbasis $\{\vec{s}_1, \vec{s}_2, \vec{s}_3 \parallel Oz\}$ from Eqs. (31)–(32), from which a parameterization $\vec{t} = [t_x, t_y, t_z = t_3]^\top$ referring to the original computational basis can readily be deduced.

In this way, as summarized by Theorem 3, the optimal input test vector $\vec{t} = \vec{t}^{\,\text{opt}}$ solving Eqs. (15)–(16) or equivalently maximizing $\|\vec{t}\,'\|^2$ in Eq. (14), is determined for any configuration of the SGAD quantum noise. The resulting maximum $\|\vec{t}\,'\| = \|\vec{t}\,'\|_{\max}$ guarantees the best performance in Eqs. (10)–(11) for minimum-error detection. Each solution $\vec{t} = \vec{t}^{\,\text{opt}}$ determines a unique optimal signaling pair $(\rho_0^{\text{opt}}, \rho_1^{\text{opt}})$ of two orthogonal pure states maximizing the performance in minimum-error detection from a noisy qubit altered by the SGAD noise in the corresponding configuration.

Theorem 3 (Optimal States for the SGAD Noise):

$$s_1 = p\left(\sqrt{1-\mu}\sqrt{1-\nu} + \sqrt{\mu\nu}\right) + (1-p)\sqrt{1-\alpha}.$$

When $s_1 > |a_{zz}|$,

if $t_z = t_z^{\text{opt}} = a_{zz}c'_z/(s_1^2 - a_{zz}^2) \in [-1, 1]$,

then $t_1^{\text{opt}} = \pm\sqrt{1 - t_z^2}$,

and $\|\vec{t}\,'\|_{\max} = s_1\sqrt{1 + c'^2_z/(s_1^2 - a_{zz}^2)}$.

if $t_z = a_{zz}c'_z/(s_1^2 - a_{zz}^2) \notin [-1, 1]$,

then $t_z^{\text{opt}} = \text{sign}(a_{zz}c'_z) = \pm 1$, $t_1^{\text{opt}} = 0$,

and $\|\vec{t}\,'\|_{\max} = |a_{zz}| + |c'_z|$.

When $s_1 \le |a_{zz}|$,

then $\vec{t}^{\,\text{opt}} = [0, 0, \text{sign}(a_{zz}c'_z) = \pm 1]^\top \parallel Oz$,

and $\|\vec{t}\,'\|_{\max} = |a_{zz}| + |c'_z|$.

□

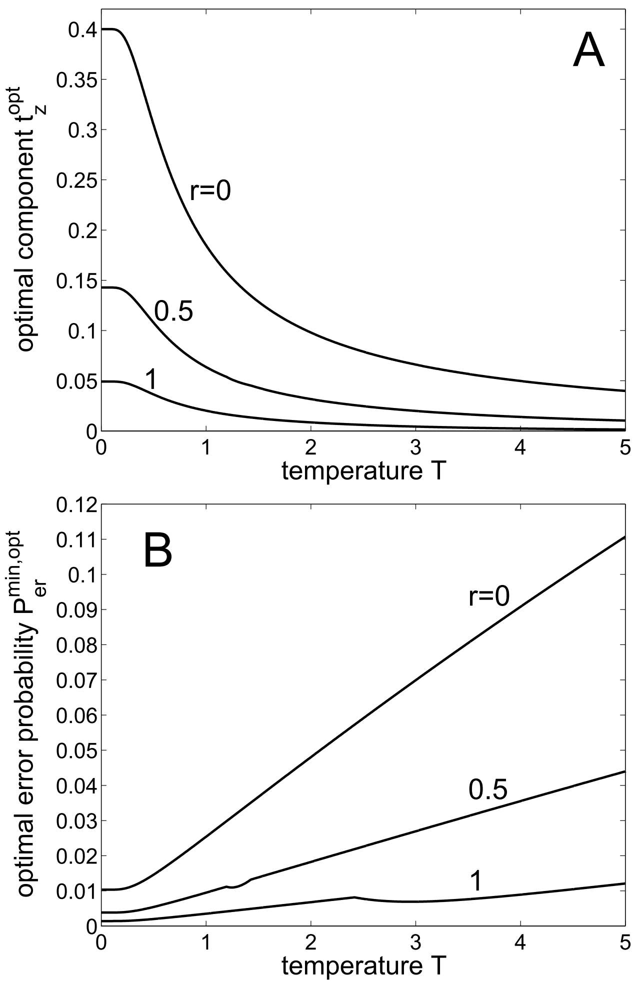

Fig. 1. For minimum-error detection from a qubit altered by a SGAD quantum noise, with prior $P_0 = 0.7$, as a function of the temperature T of the squeezed thermal bath at three values of the squeezing magnitude $r = 0$, 0.5 and 1, the optimum determined by Theorem 3 for (A) the component t_z^{opt} of the optimal input test vector $\vec{t}^{\,\text{opt}}$, and (B) the associated best performance $P_{\text{er}}^{\text{min,opt}}$ from Eqs. (10)–(11).

Theorem 3 demonstrates that for minimum-error detection, in general, both the optimal signaling pair $(\rho_0^{\text{opt}}, \rho_1^{\text{opt}})$ and the resulting best performance controlled by $\|\vec{t}\,'\|$ in Eqs. (10)–(11), are dependent upon the SGAD noise parameters and upon the prior probabilities (P_0, P_1). For illustration, Figs. 1–3 present a characterization of the optimal signaling pair and its best performance for minimum-error detection, as resulting from Theorem 3, for a SGAD noise in different configurations. In Figs. 1–3, the range of values chosen for the SGAD noise parameters, as detailed in the Appendix, are comparable to those of [19]–[21].

Figure 1 shows a characterization of the optimal signaling pair and its best performance, as a function of the temperature T of the bath, at different values of the squeezing magnitude r. Figure 1A represents the component $t_z = t_z^{\text{opt}}$ of the optimal input test vector $\vec{t}^{\,\text{opt}}$, showing that t_z^{opt} is different at each temperature T, indicating a distinct optimal signaling pair $(\rho_0^{\text{opt}}, \rho_1^{\text{opt}})$ for each temperature T of the thermal bath. As T increases in Fig. 1A, the optimal component t_z^{opt} goes

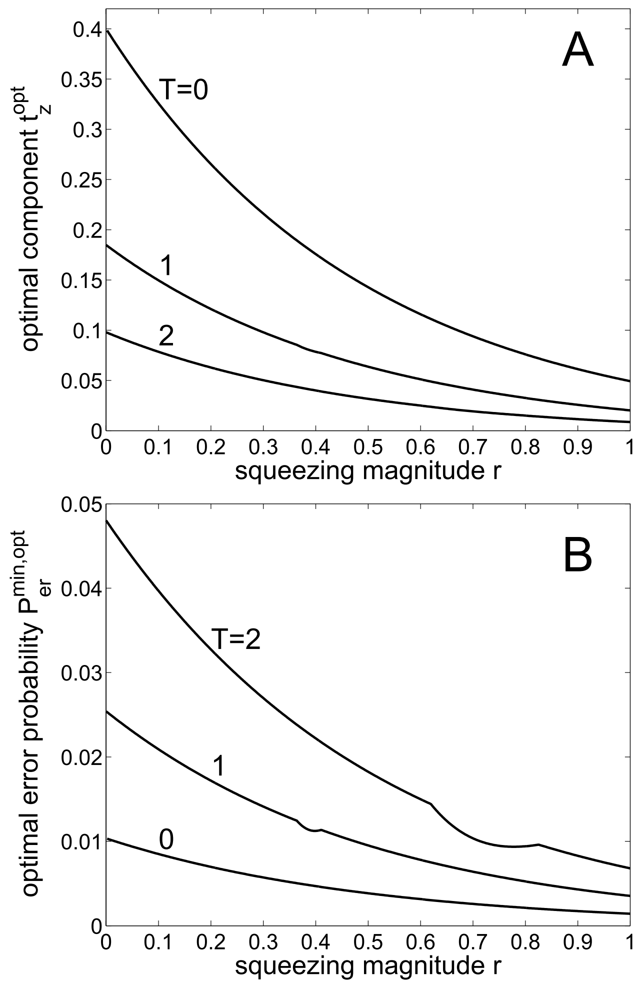

Fig. 2. For minimum-error detection from a qubit altered by a SGAD quantum noise, with prior $P_0 = 0.7$, as a function of the squeezing magnitude r of the squeezed thermal bath at three values of the temperature $T = 0$, 1 and 2, the optimum determined by Theorem 3 for (A) the component $t_z^{\rm opt}$ of the optimal input test vector $\vec{t}^{\,\rm opt}$, and (B) the associated best performance $P_{\rm er}^{\rm min,opt}$ from Eqs. (10)–(11).

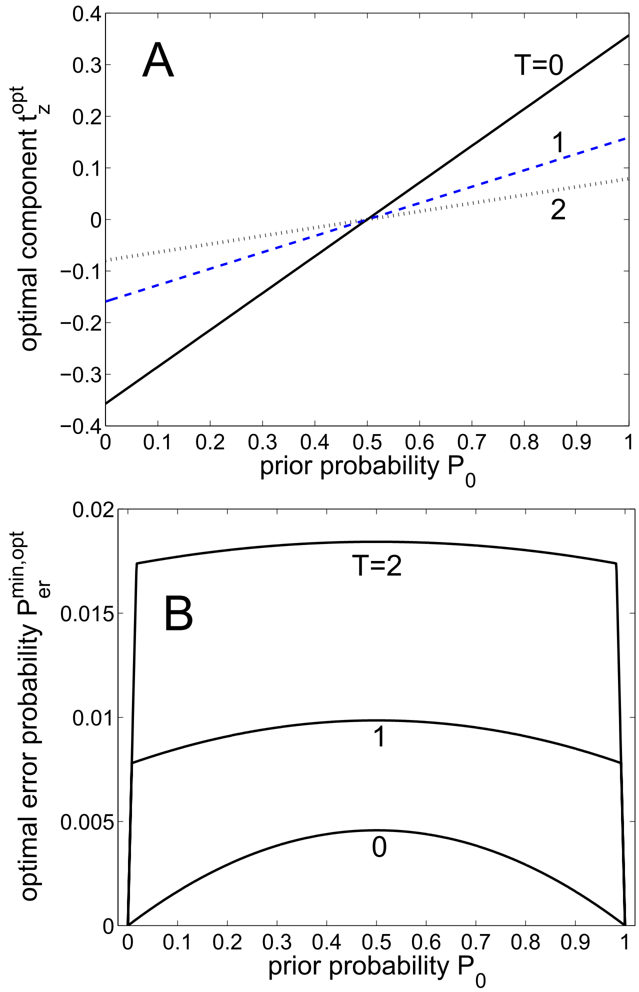

Fig. 3. For minimum-error detection from a qubit altered by a SGAD quantum noise, with squeezing magnitude $r = 0.5$, as a function of the prior probability P_0, for three values of the temperature $T = 0$, 1 and 2 of the squeezed thermal bath, the optimum determined by Theorem 3 for (A) the component $t_z^{\rm opt}$ of the optimal input test vector $\vec{t}^{\,\rm opt}$, and (B) the associated best performance $P_{\rm er}^{\rm min,opt}$ from Eqs. (10)–(11).

to zero, because in the high-temperature regime the SGAD noise evolves into a depolarizing noise, for which there is no longer a specific optimal $\vec{t}^{\,\rm opt}$, with any unit-norm $\vec{t}$ and any pair of orthogonal pure states (ρ_0, ρ_1) indifferently achieving the same performance. Figure 1B depicts the corresponding best (smallest) probability of error $P_{\rm er}^{\rm min,opt}$ in minimum-error detection, with $P_{\rm er}^{\rm min,opt}$ which is found generally to increase as the temperature T of the bath increases, as a mark of a more detrimental effect of the noise at higher temperature. Figure 1 also demonstrates that the performance in detection improves at larger squeezing magnitude r. This is a mark of the ability of squeezing of the thermal bath to counteract the detrimental effect of temperature, as also noted in [19], [20], and [23] with other performance measures. A complementary picture is given by Fig. 2 displaying $t_z^{\rm opt}$ and $P_{\rm er}^{\rm min,opt}$ as a function of the squeezing magnitude r, at different temperatures T. Figure 2A also indicates distinct $\vec{t}^{\,\rm opt}$ and optimal signaling pair $(\rho_0^{\rm opt}, \rho_1^{\rm opt})$ for each squeezing r of the thermal bath, and the corresponding performance $P_{\rm er}^{\rm min,opt}$ in Fig. 2B which generally improves as the squeezing r increases. Also in Fig. 2A, at increasing squeezing magnitude r, the optimal component $t_z^{\rm opt}$ gradually returns to zero, yielding an optimal input test vector $\vec{t}^{\,\rm opt}$ tending to $\vec{s}_1$ in Eq. (31), with $\vec{t}^{\,\rm opt}$ becoming essentially influenced by the squeezing angle Φ of the bath and no longer by the temperature T. Such behaviors, as illustrated in Figs. 1–2, offer a novel characterization of the SGAD noise, based here on the optimal conditions in minimum-error quantum detection, and conveying a complementary viewpoint on the effect of squeezing of a thermal bath and its ability to counteract the detrimental effect of temperature.

Figure 3 shows the impact of the prior probability P_0, which is found to influence both the optimal signaling pair and its best performance $P_{\rm er}^{\rm min,opt}$ for detection. Figure 3A indicates a distinct $t_z^{\rm opt}$ and therefore a distinct $\vec{t}^{\,\rm opt}$ fixing a distinct optimal signaling pair $(\rho_0^{\rm opt}, \rho_1^{\rm opt})$ for each prior probability P_0. At $P_0 = 1/2$ in Fig. 3A, one has $t_z^{\rm opt} = 0$ yielding $\vec{t}^{\,\rm opt} = \vec{s}_1$ the eigenvector of Eq. (31), as ruled by the conditions addressed in the last paragraph of Section III. Meanwhile the probability of error $P_{\rm er}^{\rm min,opt}$ is the highest at $P_0 = 1/2$, as visible in Fig. 3B, with also in general $P_{\rm er}^{\rm min,opt}$ varying with P_0.

V. Generalized Amplitude Damping Noise

With no squeezing of the thermal bath, at $r = 0$, the parameters in the Appendix yield $\mu = 0$ and $\nu = \alpha$. The SGAD quantum noise is then reduced to a generalized amplitude damping (GAD) noise [2], [22], of damping parameter $\alpha \in [0, 1]$, describing the dissipative interaction of the qubit with a standard thermal bath at temperature T, with a relaxation controlled by α towards the equilibrium mixed state $p\,|0\rangle\langle 0| + (1-p)\,|1\rangle\langle 1|$ with the probability $p \in [0, 1]$ determined by T. The GAD noise transforms the qubit state via Eq. (12) and the parameters of Eqs. (21)–(22) according to

$$\vec{r}\,' = \mathrm{A}\vec{r} + \vec{c} = \begin{bmatrix} \sqrt{1-\alpha} & 0 & 0 \\ 0 & \sqrt{1-\alpha} & 0 \\ 0 & 0 & 1-\alpha \end{bmatrix} \vec{r} + \begin{bmatrix} 0 \\ 0 \\ (2p-1)\alpha \end{bmatrix}. \tag{35}$$

We have $a_{zz} = 1-\alpha$ and $s_1 = \sqrt{1-\alpha}$, so that by Theorem 3, for the optimal input test vector, $t_z^{\rm opt} = (P_1 - P_0)(2p-1) \in [-1, 1]$. The two eigenvalues $s_1 = s_2 = s_\pm = \sqrt{1-\alpha}$ in Eq. (29) get degenerate, so any vector in the plane (Ox, Oy) is an eigenvector of A in Eq. (35), offering freedom for the two components (t_x, t_y) of the optimal $\vec{t}$ in plane (Ox, Oy). Theorem 3 then determines for the GAD noise, an optimal input test vector $\vec{t}^{\,\rm opt}$ defined by the components

$$t_z = t_z^{\rm opt} = (P_1 - P_0)(2p-1), \quad t_x^2 + t_y^2 = 1 - t_z^2, \tag{36}$$

and the solution of Eq. (36) achieves the maximum

$$\|\vec{t}\,'\|_{\max}^2 = 1 - \alpha[1 - (P_1 - P_0)^2(2p-1)^2] \tag{37}$$

to be used in Eqs. (10)–(11) to express the resulting best detection performance.

The analysis shows that $\|\vec{t}\,'\|_{\max}$ from Eq. (37) achieves in Eqs. (10)–(11) an optimal performance $P_{\rm er}^{\rm min,opt}$ which is dependent upon both noise parameters α and p. Meanwhile, the optimal signaling pair $(\rho_0^{\rm opt}, \rho_1^{\rm opt})$ determined by Eq. (36) is dependent upon the noise parameter p alone. Although this optimal pair is not unique, due to the degrees of freedom from t_x and t_y in Eq. (36), the set of optimal signaling pairs is strictly limited, and an arbitrary pair of orthogonal pure states is usually nonoptimal for detection with GAD noise.

For an illustration with a GAD noise according to Eq. (35), Fig. 4 presents the performance $P_{\rm er}^{\rm min}$ of the minimum-error detector, operating in various noise conditions and with various choices, optimal and nonoptimal, for the signaling pair (ρ_0, ρ_1).

It is clearly visible in Fig. 4 that in the presence of GAD noise, an arbitrary pair (ρ_0, ρ_1) of orthogonal pure states, like for instance $(\rho_0 = |0\rangle\langle 0|, \rho_1 = |1\rangle\langle 1|)$, is not optimal for signaling. The optimal signaling pair $(\rho_0^{\rm opt}, \rho_1^{\rm opt})$ has to be selected according to Eq. (36) so as to reach the overall minimum $P_{\rm er}^{\rm min,opt}$ of the probability of error, as shown in Fig. 4. In addition, the optimal signaling pair $(\rho_0^{\rm opt}, \rho_1^{\rm opt})$

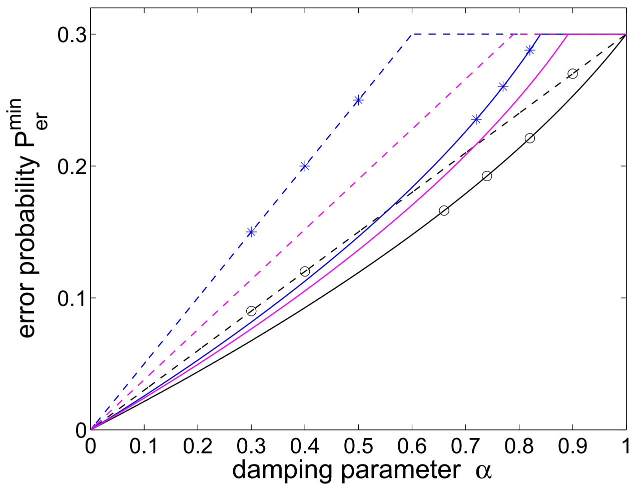

Fig. 4. For minimum-error detection from a qubit altered by a GAD noise according to Eq. (35), with prior $P_0 = 0.7$, the performance $P_{\rm er}^{\rm min}$ as a function of the damping parameter α, for three values of the noise probability p: (∘) $p = 0$, (∗) $p = 0.5$, (no mark) $p = 0.2$. The solid lines show the overall best performance $P_{\rm er}^{\rm min,opt}$ of Eqs. (10)–(11) when the detector operates with the optimal signaling pair $(\rho_0^{\rm opt}, \rho_1^{\rm opt})$ determined by Eq. (36). Associated with each solid line is a dotted line showing $P_{\rm er}^{\rm min}$ with the fixed nonoptimal signaling pair $(\rho_0 = |0\rangle\langle 0|, \rho_1 = |1\rangle\langle 1|)$.

achieving $P_{\rm er}^{\rm min,opt}$ in Fig. 4 is distinct for each value of p, following Eq. (36). This, in practice, means a distinct optimal signaling pair for each temperature T of the thermal bath representing the environment. Yet, for a given p the optimal signaling pair is invariant with the damping parameter α. In a quantum communication framework, the signaling and detection stages can thus be kept fixed at given p for any α. The optimal performance $P_{\rm er}^{\rm min,opt}$ however degrades with increasing damping α, as visible in Fig. 4.

VI. Quantum Pauli Noise

Another broad class of quantum noise which can affect a qubit and that is not represented by the SGAD noise model of Section IV is the Pauli noise [2], [3]. It acts through random applications of the four Pauli operators $\{\sigma_0 = \mathbb{1}, \sigma_x, \sigma_y, \sigma_z\}$, which form an orthogonal basis for operators on $\mathcal{H}_2$. It can be described by a Kraus representation according to Eq. (8) as

$$\rho' = \mathcal{N}(\rho) = \sum_{k=0,x,y,z} p_k \sigma_k \rho \sigma_k^\dagger, \tag{38}$$

with the $\{p_k\}$ a probability distribution. The linear transformation of Eq. (38) always satisfying $\mathcal{N}(\mathbb{1}) = \mathbb{1}$ belongs to the class of unital noise channels for the qubit, with specific interesting properties [24], [25]. The resulting transformation of the qubit Bloch vector in Eq. (12) follows as

$$\vec{r}\,' = \mathrm{A}\vec{r} = \begin{bmatrix} a_x & 0 & 0 \\ 0 & a_y & 0 \\ 0 & 0 & a_z \end{bmatrix} \vec{r}, \tag{39}$$

with the real scalar coefficients

$$a_x = p_0 + p_x - p_y - p_z, \tag{40}$$

$$a_y = p_0 - p_x + p_y - p_z, \tag{41}$$

$$a_z = p_0 - p_x - p_y + p_z. \tag{42}$$

Since A in Eq. (39) is in diagonal form, then $\mathrm{A} \equiv \mathrm{S}$, and according to Theorems 1 and 2, maximization of $\|\vec{t}\,'\|^2$ in Eq. (14) is achieved by placing in $\vec{t} = \vec{t}^{\,\mathrm{opt}}$ a single unit component $|t_k| = 1$ in the direction k such that

$$|a_k| = \max(|a_x|, |a_y|, |a_z|), \tag{43}$$

so as to achieve the maximum $\|\vec{t}\,'\|_{\max} = |a_k|$ to be used in Eqs. (10)–(11) to express the best detection performance.

For an illustration with a Pauli noise process according to Eq. (38), we consider the Kraus representation in Eq. (38) under the form

$$\mathcal{N}(\rho) = (1-p)\rho + p\left(1 - \frac{2}{3}q\right)\sigma_x \rho \sigma_x^\dagger + \frac{1}{3}pq\left(\sigma_y \rho \sigma_y^\dagger + \sigma_z \rho \sigma_z^\dagger\right), \tag{44}$$

with a parameter $q \in [0, 1]$. The noise model of Eq. (44) is a convex combination interpolating between a bit-flip noise at $q = 0$, and a depolarizing noise at $q = 1$. For any q between 0 and 1, Eq. (44) gives access to a valid quantum noise, enabling to represent a whole range of quantum noises in a tunable way, as exploited for instance in [26] and [27]. In Eq. (44), with probability $1-p$ the state ρ is left unchanged, while ρ is changed with probability p by application of one or the other of the three Pauli operators. The corresponding coefficients of Eqs. (40)–(42) become

$$a_x = 1 - \frac{4}{3}pq, \tag{45}$$

$$a_y = a_z = 1 - 2p + \frac{2}{3}pq. \tag{46}$$

For a given q fixing the noise type in Eq. (44), the condition of Eq. (43) determines a specific optimal pair $(\rho_0^{\mathrm{opt}}, \rho_1^{\mathrm{opt}})$ of signaling states according to the probability p of action of the quantum noise.

For $0 \leq p \leq 3/(3+q)$, the solution of Eq. (43) is $|a_k| = |a_x|$ with an optimal $\vec{t}$ which is $\vec{t}^{\,\mathrm{opt}} = [t_x = 1, t_y = 0, t_z = 0]^\top$. This defines the optimal signaling pair $(\rho_0^{\mathrm{opt}} = |-\rangle\langle -|, \rho_1^{\mathrm{opt}} = |+\rangle\langle +|)$ with the two orthogonal pure states $|+\rangle = (|0\rangle + |1\rangle)/\sqrt{2}$ and $|-\rangle = (|0\rangle - |1\rangle)/\sqrt{2}$. Note that $\vec{t}^{\,\mathrm{opt}} = [t_x = -1, t_y = 0, t_z = 0]^\top$ defines the other optimal solution, with the optimal signaling pair $(\rho_0^{\mathrm{opt}} = |+\rangle\langle +|, \rho_1^{\mathrm{opt}} = |-\rangle\langle -|)$, and equivalent performance controlled by $\|\vec{t}\,'\|_{\max} = |a_x|$ in Eqs. (10)–(11).

For $3/(3+q) \leq p \leq 1$, a solution of Eq. (43) is $|a_k| = |a_z|$ with an optimal $\vec{t}$ which can be taken as $\vec{t}^{\,\mathrm{opt}} = [t_x = 0, t_y = 0, t_z = 1]^\top$. This defines the optimal signaling pair $(\rho_0^{\mathrm{opt}} = |1\rangle\langle 1|, \rho_1^{\mathrm{opt}} = |0\rangle\langle 0|)$. Note that any $\vec{t} = [t_x = 0, t_y \neq 0, t_z \neq 1]^\top$ with $t_y^2 + t_z^2 = 1$ defines another optimal solution $\vec{t}^{\,\mathrm{opt}}$ with equivalent performance controlled by $\|\vec{t}\,'\|_{\max} = |a_z|$ in Eqs. (10)–(11).

Figure 5 illustrates some generic properties of the optimal configurations for minimum-error detection with Pauli noise. Usually, both the optimal signaling pair $(\rho_0^{\mathrm{opt}}, \rho_1^{\mathrm{opt}})$ determined by $\vec{t}^{\,\mathrm{opt}}$ and its performance $P_{\mathrm{er}}^{\mathrm{min,opt}}$ are dependent upon the Pauli noise type and noise level, as represented by q and p in Fig. 5. By contrast, the optimality condition of Eq. (43) shows that the optimal signaling pair $(\rho_0^{\mathrm{opt}}, \rho_1^{\mathrm{opt}})$ is independent of the prior probabilities (P_0, P_1), while the associated overall best performance $P_{\mathrm{er}}^{\mathrm{min,opt}}$ depends on (P_0, P_1) only via the position of $\|\vec{t}\,'\|_{\max} = |a_k|$ relative to $|P_1 - P_0|$ in Eqs. (10)–(11). As a result, for $P_0 \neq 1/2$, the curves of $P_{\mathrm{er}}^{\min}$ of Fig. 5 still apply but have to be limited at $\min(P_0, P_1)$ according to Eq. (11) when $\|\vec{t}\,'\|_{\max} = |a_k| < |P_1 - P_0|$, in which condition the minimum-error detector characterized in Section II need not use any measurement and always decides for the the state with maximum prior probability. Beyond the illustrative conditions of Fig. 5, the solution of this Section allows one to track the optimal signaling pair $(\rho_0^{\mathrm{opt}}, \rho_1^{\mathrm{opt}})$ matched to any noise level and any Pauli noise according to Eq. (38), so as to optimize minimum-error detection from the noisy qubit.

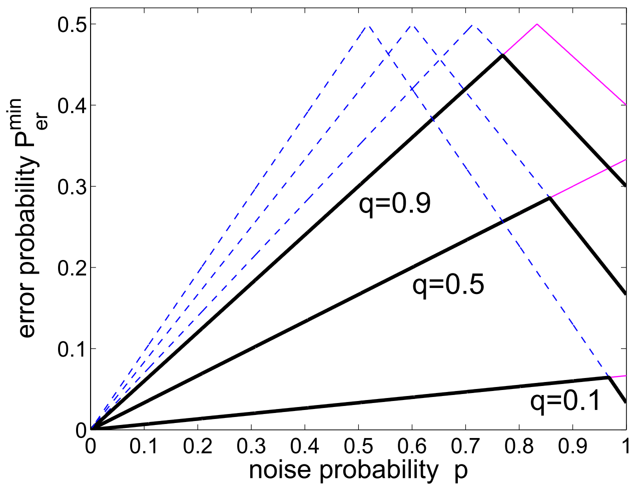

Fig. 5. For minimum-error detection from a qubit altered by a Pauli quantum noise of Eq. (44), with prior $P_0 = 1/2$, the performance $P_{\mathrm{er}}^{\min}$ as a function of the probability p of action of the noise, for three values of q fixing the type of the noise. For each q, the thick (black) line is the overall best performance $P_{\mathrm{er}}^{\mathrm{min,opt}}$ of Eqs. (10)–(11) when the detector operates with the optimal signaling pair $(\rho_0^{\mathrm{opt}}, \rho_1^{\mathrm{opt}})$ defined from Eq. (43). Associated with each thick line are two thin lines showing $P_{\mathrm{er}}^{\min}$ with the fixed signaling pair $(\rho_0 = |-\rangle\langle -|, \rho_1 = |+\rangle\langle +|)$ (dotted (blue) line), and $(\rho_0 = |1\rangle\langle 1|, \rho_1 = |0\rangle\langle 0|)$ (solid (magenta) line), each of these two pairs ceasing to be optimal respectively for p below or above $3/(3+q)$.

VII. One Imposed Signaling State

Another situation is when one of the signaling state, say ρ_0, is fixed and imposed. One then seeks the other signaling state ρ_1 in order to maximize the performance in minimum-error detection as before. The transformed test vector of Eq. (13) can then be written as $\vec{t}\,' = P_1 \mathrm{A} \vec{r}_1 + \vec{c}\,''$, and its squared norm of Eq. (14) can conveniently be expressed as

$$\|\vec{t}\,'\|^2 = \|P_1 \mathrm{A} \vec{r}_1\|^2 + 2\vec{w}^{\top}\vec{r}_1 + \|\vec{c}\,''\|^2, \tag{47}$$

with the vectors $\vec{c}\,'' = \vec{c}\,' - P_0 \mathrm{A} \vec{r}_0$ and $\vec{w} = P_1 \mathrm{A}^\top \vec{c}\,''$ both given when ρ_0, i.e. $\vec{r}_0$, is given. The task is then to find $\vec{r}_1$, subject to the constraint $\|\vec{r}_1\| \leq 1$, maximizing $\|\vec{t}\,'\|^2$ of Eq. (47). The maximum of $\|\vec{t}\,'\|^2$ in Eq. (47) occurs at the saturated constraint $\|\vec{r}_1\| = 1$, by the same argument as in the proof of Theorem 1. This indicates a pure signaling state ρ_1 which is optimal for minimum-error detection in association with any, pure or mixed, imposed state ρ_0. Since Eq. (47) has a form similar to Eq. (14), further characterization of $\vec{r}_1$ maximizing $\|\vec{t}\,'\|^2$ in Eq. (47), can be obtained as in Theorem 2. For a fixed $\vec{r}_0$, this will produce an optimal solution $\vec{r}_1 = \vec{r}_1^{\,\mathrm{opt}}$ not parallel to $\vec{r}_0$ in general, therefore an optimal pure signaling state ρ_1^{opt} not orthogonal to the other imposed signaling state ρ_0.

For example, ρ_0 can be imposed as the maximally mixed state $\rho_0 = \mathbb{1}/2$, of $\vec{r}_0 = \vec{0}$, which is an invariant state for any Pauli noise according to Eqs. (38)–(39). In this case, with Pauli noise, the associated optimal signaling state ρ_1^{opt} is determined by $\vec{r}_1 = \vec{r}_1^{\,\mathrm{opt}} = \vec{t}^{\,\mathrm{opt}}$, where $\vec{t}^{\,\mathrm{opt}}$ is the optimal test vector obtained in Section VI via Eq. (43), yet with a performance controlled by $\|\vec{t}\,'\|_{\max}$ in Eqs. (10)–(11) which is reduced by the multiplicative factor $P_1 \le 1$ as the cost incurred by imposing the (non-optimal) signaling state $\rho_0 = \mathbb{1}/2$.

As another example, one can impose the pure signaling state $\rho_0 = |0\rangle\langle 0|$, of $\vec{r}_0 = [0, 0, 1]^\top$, for detection in the SGAD noise of Section IV. Then $\vec{c}\,''$ introduced in Eq. (47) is $\vec{c}\,'' = [0, 0, c''_z = c'_z - P_0 a_{zz}]^\top$ and remains parallel to Oz, preserving the geometry underlying the maximization of Eqs. (33)–(34), with a criterion becoming $J(\vec{r}_1) = P_1^2 s_1^2 r_{1,1}^2 + P_1^2 a_{zz}^2 r_{1,z}^2 + 2P_1 a_{zz} c''_z r_{1,z}$ to be maximized according to $\vec{r}_1$ under $\|\vec{r}_1\| = 1$. This is the same form of maximization which is solved by Theorem 3, allowing to predict, in generic conditions, a solution $\vec{r}_1^{\,\mathrm{opt}}$ with components both along Oz and in the plane (Ox, Oy) orthogonal to Oz, i.e. an optimal signaling state ρ_1^{opt} not orthogonal to the other imposed signaling state $\rho_0 = |0\rangle\langle 0|$.

VIII. Conclusion

We have addressed minimum-error detection from a qubit altered by an arbitrary quantum noise. The noise is separately characterized and modeled as a channel performing an input–output transformation to the qubit. Optimization of the pair of input signaling states is addressed so as to match the noise properties and achieve the best performance in minimum-error detection from the noisy qubit accessible as the output of the noise channel. This separate account of the noise is a specificity here of the approach to detection, because usually for quantum detection or quantum state discrimination, the noisy states are generally treated as mixed states, but with no explicit consideration, in the derivation of the optimal processings, of the underlying noise producing the mixed states.

For an arbitrary quantum noise affecting the qubit, we have obtained a general characterization of the optimal pairs of signaling states and the best performance they achieve for minimum-error detection from the noisy qubit. This characterization takes the form of a simple maximization of a real scalar quadratic criterion in three real scalar variables limited by an equality constraint, as expressed by Theorem 2, the solutions of which determine the optimal signaling pairs and their best performance. This general characterization allowed us to prove, as stated by Theorem 1, that the optimal signaling pairs are always formed of two orthogonal pure quantum states, but that must be specifically matched to the noise. Also the general characterization, via the role of $\vec{c}\,'$ and $\vec{v}$ in Eqs. (14) and (15), shows that the prior probabilities of the two signaling states generally influence the optimal signaling pairs and their best performance. These given prior probabilities specify the detection problem and its optimal solutions in contrast to other transmission problems where the prior probabilities are variable parameters which can be adjusted in the optimization process, as is the case in the determination of various information capacities for quantum channels [19], [28], [29]. In such cases the optimal solutions often occur with equiprobable priors, while for detection here the necessity of handling skewed nonequiprobable priors usually makes more complicated the determination of the optimum yet to also achieve usually higher performance in detection, as for instance illustrated in Fig. 3.

For several generic quantum noise processes relevant to the qubit, the maximization problem of Theorem 2 has been solved explicitly. Especially, the optimal solutions have been exhibited for the squeezed generalized amplitude damping noise. This in particular offered a novel characterization for this quantum noise, based on optimal detection conditions, and materialized by increased squeezing entailing improved detection, confirming with another approach the ability of squeezing to counteract the detrimental action of a thermal bath representing a decohering environment. Also the solutions here included as special cases both the generalized and the regular amplitude damping noises, with in addition the Pauli noise treated separately, to cover a large class of noise processes that can practically affect a qubit.

The present approach to quantum detection optimized for a specific noise process can be extended in several directions. One can consider extensions to discrimination of more than two qubit states [30], [31], or to quantum systems with dimension higher than the dimension two of the qubit [32], [33], or to performance measures other than the probability of error in discrimination [10], [11], [15], [34]. Yet it is known that such extended conditions are usually more difficult to handle analytically, with general solutions not necessarily accessible theoretically, especially with a separate characterization of the quantum noise which demands broader prior determination of the problem. By contrast, the situation of detection on the qubit can be solved analytically in detail, as undertaken here, and offers in this way the guideline of a basic setting where complete theoretical resolution can be performed and which can be useful for further development in quantum signal processing.

Appendix

The SGAD quantum noise [19]–[21] acting on the qubit through Eqs. (8) and (17)–(20), results from a qubit coupled to an environment formed by a squeezed thermal bath at temperature T. Squeezing of a thermal bath is obtained by a nonlinear operation capable of introducing correlations between the modes or thermal photons of the bath, with possibilities of reducing the decoherence of quantum states. The effect of the squeezed thermal bath on the qubit can be expressed through a squeezing operator [19]–[21]

$$\mathrm{R} = \sigma_- \cosh(r) + e^{i\Phi}\sigma_+ \sinh(r), \tag{A-1}$$

performing a squeezing transformation [35] characterized by a magnitude r and phase Φ, and acting on the standard lowering and raising operators, respectively $\sigma_- = |0\rangle\langle 1| = (\sigma_x - i\sigma_y)/2$ and $\sigma_+ = |1\rangle\langle 0| = (\sigma_x + i\sigma_y)/2$. The squeezing operator R of Eq. (A-1) determines the Lindblad operators acting in the Lindblad equation governing the evolution of the state ρ of the qubit interacting with the squeezed thermal bath. Resolution of this Lindblad linear differential equation then leads to the expressions of the Kraus operators of Eqs. (17)–(20) for the evolution of the qubit state ρ. The parameters defining the Kraus operators of Eqs. (17)–(20), and summarizing the interaction with the squeezed thermal bath, result as [19]–[21]

$$\nu = \frac{N}{p(2N+1)}\Big(1 - \exp[-\gamma_0(2N+1)t]\Big), \tag{A-2}$$

$$\mu = \frac{2N+1}{2pN}\frac{\sinh^2(\gamma_0 a t/2)}{\sinh[\gamma_0(2N+1)t/2]}\exp\Big[-\frac{\gamma_0}{2}(2N+1)t\Big], \tag{A-3}$$

$$\alpha = \frac{1}{1-p}\Big(1 - p(\mu+\nu) - \exp[-\gamma_0(2N+1)t]\Big). \tag{A-4}$$

In Eqs. (A-2)–(A-4), γ_0 is the spontaneous emission rate of photons in the bath, t is the time duration of the interaction of the qubit with the bath, $N = [\cosh^2(r) + \sinh^2(r)]\, N_{\rm th} + \sinh^2(r)$ is related to the number of thermal photons $N_{\rm th} = 1/[\exp(\hbar\omega/k_B T) - 1]$ given by the Planck distribution at frequency ω, and $a = (2N_{\rm th}+1)\sinh(2r)$. There is also the probability

$$\begin{aligned} p = p_\pm = {} & \frac{1}{(A+B-C-1)^2 - 4D} \\ & \times\Big(A^2B + C^2 + A[B^2 - C - B(1+C) - D] \\ & \quad - (1+B)D - C(B+D-1) \\ & \quad \pm 2\sqrt{\begin{aligned}&D[B - AB + (A-1)C + D]\\ &\times[(A - AB + (B-1)C + D]\end{aligned}}\Big), \end{aligned} \tag{A-5}$$

with either sign $\pm$ in Eq. (A-5) leading to a valid SGAD noise (p_- is used in the examples of Figs. 1–3), and with [19]–[21]

$$A = \frac{2N+1}{2N}\frac{\sinh^2(\gamma_0 a t/2)}{\sinh[\gamma_0(2N+1)t/2]}\exp[-\gamma_0(2N+1)t/2], \tag{A-6}$$

$$B = \frac{N}{2N+1}\Big(1 - \exp[-\gamma_0(2N+1)t]\Big), \tag{A-7}$$

$$C = A + B + \exp[-\gamma_0(2N+1)t], \tag{A-8}$$

$$D = \cosh^2(\gamma_0 a t/2)\exp[-\gamma_0(2N+1)t]. \tag{A-9}$$

In the illustrations of Figs. 1–3, the parameters of the SGAD noise are expressed in units where $\hbar\omega/k_B = 1$, with a spontaneous photon emission rate $\gamma_0 = 0.05$, an interaction time $t = 1$ of the qubit with the bath, and over ranges of the temperature T and squeezing magnitude r, to reproduce conditions comparable to those of [19]–[21].

Several regimes of operation have special physical significance for the SGAD quantum noise. At large interaction time $t \to \infty$, the probability $p \to p(t=\infty) = (N+1)/(2N+1)$, and the qubit relaxes to the asymptotic mixed state $p(t=\infty)|0\rangle\langle 0| + [1 - p(t=\infty)]|1\rangle\langle 1|$ controlled by the temperature T and squeezing magnitude r of the bath. Otherwise, when the squeezing magnitude $r = 0$, the SGAD noise is reduced to a generalized amplitude damping noise [2], [22] with damping parameter $\alpha \in [0,1]$ and a time-independent probability $p \in [0,1]$, describing the dissipative coupling of the qubit to a standard thermal bath at finite temperature T and relaxing to the mixed state $p|0\rangle\langle 0| + (1-p)|1\rangle\langle 1|$; and when in addition $T = 0$, the SGAD noise is further reduced to a standard amplitude damping noise [2], [36], with a probability $p = 1$, describing relaxation of the qubit to the ground state $|0\rangle\langle 0|$ by equilibration with a vacuum bath. Otherwise, at large temperature $T \to \infty$, then the probability $p \to p(T=\infty) = 1/2$, and the SGAD noise is reduced to a fully depolarizing noise [2], with a qubit driven to the maximally mixed state $\mathbb{1}/2$.

References

[1] C. H. Bennett and P. W. Shor, "Quantum information theory," *IEEE Trans. Inf. Theory*, vol. 44, no. 6, pp. 2724–2742, Oct. 1998.

[2] M. A. Nielsen and I. L. Chuang, *Quantum Computation and Quantum Information*. Cambridge, U.K.: Cambridge Univ. Press, 2000.

[3] M. M. Wilde, *Quantum Information Theory*. Cambridge, U.K.: Cambridge Univ. Press, 2013.

[4] C. W. Helstrom, "Quantum detection and estimation theory," *J. Statist. Phys.*, vol. 1, no. 2, pp. 231–252, 1969.

[5] A. S. Holevo, "Statistical decision theory for quantum systems," *J. Multivariate Anal.*, vol. 3, no. 4, pp. 337–394, 1973.

[6] C. W. Helstrom, Ed., *Quantum Detection and Estimation Theory*. New York, NY, USA: Academic, 1976.

[7] M. Osaki, M. Ban, and O. Hirota, "Derivation and physical interpretation of the optimum detection operators for coherent-state signals," *Phys. Rev. A*, vol. 54, pp. 1691–1701, Aug. 1996.

[8] A. Chefles, "Unambiguous discrimination between linearly independent quantum states," *Phys. Lett. A*, vol. 239, no. 6, pp. 339–347, 1998.

[9] T. Rudolph, R. W. Spekkens, and P. S. Turner, "Unambiguous discrimination of mixed states," *Phys. Rev. A*, vol. 68, pp. 010301(R)-1–010301(R)-4, Jul. 2003.

[10] U. Herzog and J. A. Bergou, "Distinguishing mixed quantum states: Minimum-error discrimination versus optimum unambiguous discrimination," *Phys. Rev. A*, vol. 70, pp. 022302-1–022302-6, Aug. 2004.

[11] Y. C. Eldar and G. D. Forney, Jr., "On quantum detection and the square-root measurement," *IEEE Trans. Inf. Theory*, vol. 47, no. 3, pp. 858–872, Mar. 2001.

[12] Y. C. Eldar, A. Megretski, and G. C. Verghese, "Designing optimal quantum detectors via semidefinite programming," *IEEE Trans. Inf. Theory*, vol. 49, no. 4, pp. 1007–1012, Apr. 2003.

[13] Y. C. Eldar, A. Megretski, and G. C. Verghese, "Optimal detection of symmetric mixed quantum states," *IEEE Trans. Inf. Theory*, vol. 50, no. 6, pp. 1198–1207, Jun. 2004.

[14] M. A. Ballester, S. Wehner, and A. Winter, "State discrimination with post-measurement information," *IEEE Trans. Inf. Theory*, vol. 54, no. 9, pp. 4183–4198, Sep. 2008.

[15] K. Nakahira, K. Kato, and T. S. Usuda, "Minimax strategy in quantum signal detection with inconclusive results," *Phys. Rev. A*, vol. 88, pp. 032314-1–032314-9, Sep. 2013.

[16] O. Oreshkov, J. Calsamiglia, R. Muñoz-Tapia, and E. Bagan, "Optimal signal states for quantum detectors," *New J. Phys.*, vol. 13, no. 7, pp. 073032-1–073032-22, 2011.

[17] N. Elron and Y. C. Eldar, "Optimal encoding of classical information in a quantum medium," *IEEE Trans. Inf. Theory*, vol. 53, no. 5, pp. 1900–1907, May 2007.

[18] A. Pasieka, D. W. Kribs, R. Laflamme, and R. Pereira, "On the geometric interpretation of single qubit quantum operations on the Bloch sphere," *Acta Appl. Math.*, vol. 108, no. 3, pp. 697–707, 2009.

[19] R. Srikanth and S. Banerjee, "Squeezed generalized amplitude damping channel," *Phys. Rev. A*, vol. 77, p. 012318, Jan. 2008.

[20] S. Banerjee and R. Srikanth, "Geometric phase of a qubit interacting with a squeezed-thermal bath," *Eur. Phys. J. D*, vol. 46, no. 2, pp. 335–344, 2008.

[21] S. Omkar, R. Srikanth, and S. Banerjee, "Dissipative and non-dissipative single-qubit channels: Dynamics and geometry," *Quantum Inf. Process.*, vol. 12, no. 12, pp. 3725–3744, 2013.

[22] C. Cafaro and P. van Loock, "Approximate quantum error correction for generalized amplitude-damping errors," *Phys. Rev. A*, vol. 89, p. 022316, Feb. 2014.

[23] S. Banerjee and R. Srikanth, "Phase diffusion in quantum dissipative systems," *Phys. Rev. A*, vol. 76, p. 062109, Dec. 2007.

[24] C. King and M. B. Ruskai, "Minimal entropy of states emerging from noisy quantum channels," *IEEE Trans. Inf. Theory*, vol. 47, no. 1, pp. 192–209, Jan. 2001.

[25] C. King, "Additivity for unital qubit channels," *J. Math. Phys.*, vol. 43, no. 10, pp. 4641–4653, 2002.

[26] G. Bowen and S. Mancini, "Stochastic resonance effects in quantum channels," *Phys. Lett. A*, vol. 352, nos. 4–5, pp. 272–275, 2006.

[27] F. Chapeau-Blondeau, "Quantum state discrimination and enhancement by noise," *Phys. Lett. A*, vol. 378, nos. 30–31, pp. 2128–2136, 2014.

[28] E. Davies, "Information and quantum measurement," *IEEE Trans. Inf. Theory*, vol. 24, no. 5, pp. 596–599, Sep. 1978.

[29] A. S. Holevo, "The capacity of the quantum channel with general signal states," *IEEE Trans. Inf. Theory*, vol. 44, no. 1, pp. 269–273, Jan. 1998.

[30] H. P. Yuen, R. S. Kennedy, and M. Lax, "Optimum testing of multiple hypotheses in quantum detection theory," *IEEE Trans. Inf. Theory*, vol. 21, no. 2, pp. 125–134, Mar. 1975.

[31] J. Bae and W.-Y. Hwang, "Minimum-error discrimination of qubit states: Methods, solutions, and properties," *Phys. Rev. A*, vol. 87, p. 012334, Jan. 2013.

[32] S. M. Barnett and S. Croke, "Quantum state discrimination," *Adv. Opt. Photon.*, vol. 1, no. 2, pp. 238–278, 2009.

[33] J. Bae, "Structure of minimum-error quantum state discrimination," *New J. Phys.*, vol. 15, pp. 073037-1–073037-31, Jul. 2013.

[34] S. Croke, E. Andersson, S. M. Barnett, C. R. Gilson, and J. Jeffers, "Maximum confidence quantum measurements," *Phys. Rev. Lett.*, vol. 96, pp. 070401-1–070401-4, Feb. 2006.

[35] Y. S. Kim and M. E. Noz, "Lorentz harmonics, squeeze harmonics and their physical applications," *Symmetry*, vol. 3, no. 1, pp. 16–36, 2011.

[36] S.-T. Wu, "Quenched decoherence in qubit dynamics due to strong amplitude-damping noise," *Phys. Rev. A*, vol. 89, p. 034301, Mar. 2014.

François Chapeau-Blondeau was born in France in 1959. He received the Engineer Diploma from ESEO, Angers, France, in 1982, the Ph.D. degree in electrical engineering from University Pierre et Marie Curie, Paris 6, France, in 1987, and the Habilitation degree from the University of Angers, France, in 1994. In 1988, he was a research associate in the Department of Biophysics at the Mayo Clinic, Rochester, Minnesota, USA, working on biomedical ultrasonics. Since 1990, he has been with the University of Angers, France, where he is currently a professor of electrical and electronic engineering. His research interests include information theory, signal processing and imaging, and the interactions between physics and information sciences.